Continuous electrowetting at the low concentration electrolyte-insulator-semiconductor junction

S. Arscott

Applied Physics Letters

Continuous electrowetting at the low concentration electrolyte-insulator-semiconductor junction

Cite as: Appl. Phys. Lett. **105**, 231604 (2014); https://doi.org/10.1063/1.4903513
Submitted: 24 July 2014 • Accepted: 23 November 2014 • Published Online: 08 December 2014

Steve Arscott

Continuous electrowetting at the low concentration electrolyte-insulator-semiconductor junction

Steve Arscott[a)]
Institut d'Electronique, de Microélectronique et de Nanotechnologie (IEMN), CNRS UMR8520, The University of Lille, Cité Scientifique, Avenue Poincaré, 59652 Villeneuve d'Ascq, France

(Received 24 July 2014; accepted 23 November 2014; published online 8 December 2014)

Electrowetting (EW) has applications including displays, microactuation, miniaturized chemistry, adaptive optics, and energy harvesting—understanding the physics of EW junctions is of key importance. Here, the roles of semiconductor space-charge and electric double layer in continuous EW at an electrolyte-insulator-semiconductor junction are considered. A model is formulated in terms of experimental parameters—applied voltage, zero-bias wetting contact angle, semiconductor type and doping, insulator thickness and dielectric constant, and electrolyte concentration and dielectric constant. The model predicts, and experiments indicate, that the EW behavior is diminished for low concentration solutions (~1–10 nM) and lowly doped silicon (10^{14}–10^{15} cm^{-3}).
 [http://dx.doi.org/10.1063/1.4903513]

Electrowetting[1,2] (EW) applications[3–13] range from microactuation[13] to miniaturized chemistry,[12] where the electrical conductivity of the liquid varies from $\sim 10^{6}$ to $\sim 10^{-6}$ S m^{-1}. Early continuous EW experiments[14–16]—using electrolyte concentrations typically above the mM range—concluded that the EW depended little on electrolyte concentration. However, subsequent experiments[17–21] have revealed the influence of electric double layer[22] (EDL) at lower concentrations. Continuous EW can also be observed using semiconductors,[23–26] e.g., at the electrolyte-insulator-semiconductor (EIS) junction[23]—EIS junctions have many applications,[27–30] as do semiconductor-dielectric hybrid devices,[31] which could potentially benefit from a link with EW. Thus, an understanding of the influence of the EDL in EW is of importance, especially in EW applications involving low concentration samples, e.g., laboratory-on-a-chip mass spectrometry.[12]

The Young-Lippmann equation[1] for EW of a droplet resting on a surface is

$$\cos\theta = \cos\theta_0 + \frac{E}{\gamma}, \tag{1}$$

where θ is the macroscopic contact angle, θ_0 is the zero-bias contact angle, E is the stored electrical energy in the system—due to the applied external voltage—and γ is the liquid-vapor surface energy (i.e., the surface tension of the liquid) of the liquid. By considering the effects of space-charge in the semiconductor and the EDL on EW at an EIS junction, we are supposing that an electric field is present in the space-charge, the insulator, and the liquid—but only at the electrolyte-solid interface. Dielectric liquids (e.g., solvents, oils, etc.), where the electric field is present in the liquid, are actuated by dielectrophoresis.[32] At relatively low voltages (<1 V), the capacitance of an EDL can be described by well-known formulae[22]—although the subject is still a matter of ongoing research.[33] This has enabled the development of electrical models[34,35] for the EIS junction which work well for most low-voltage applications involving ISFETs. In contrast, even recent low-voltage[36,37] EW requires applied voltages which are much larger than 1 V implying that the low-voltage EDL model cannot be used to describe EW at an EIS junction—to solve this, one has to look at work concerning EDL at higher voltages, i.e., >1 V.[38–43]

We can consider the EIS junction to be three perfect capacitances (lossless) connected in series: one associated with the semiconductor space-charge, one associated with the insulator, and one associated with the whole EDL—see inset to Fig. 1

$$V = V_{sc} + V_i + V_e, \tag{2}$$

$$Q_{sc} = Q_i = Q_e, \tag{3}$$

where V is the applied external voltage and V_{sc}, V_i, and V_e are the potential differences across the space-charge, the insulator, and the entire EDL. We do not consider here the small voltage drop at the ideal electrode completing the circuit.[1] We consider that V does not incur breakdown in the semiconductor or the insulator and that the applied frequency is low.[44] The charge associated with a depleted semiconductor Q_{sc} can be approximated using the following equation:[44]

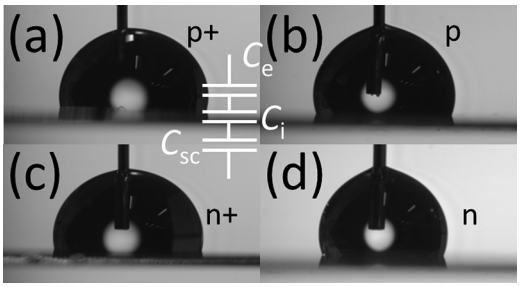

FIG. 1. EW at an EIS junction—effect of semiconductor doping. (a) p+ type silicon using at +25 V, (b) p-type at +25 V, (c) n+ type at −25 V, and (d) n-type silicon at −25 V. The solution concentration is 10 mM and the insulator is a 265 nm thick amorphous fluoropolymer (Teflon®AF). The diameter of the needle is 300 μm. The inset shows the series capacitor model composed of the EDL capacitance (C_e), the dielectric capacitance (C_i), and the space-charge capacitance (C_{sc}) in the semiconductor.

a)Electronic mail: steve.arscott@iemn.univ-lille1.fr . Tel.: +33 320197979.

$$Q_{sc} \approx \alpha\sqrt{V_{sc}}, \tag{4}$$

$$\alpha = \sqrt{2q\varepsilon_{sc}\varepsilon_0 N}, \tag{5}$$

where q is the elementary charge (1.6×10^{-19} C), ε_{sc} is the dielectric constant of the semiconductor (e.g., 11.9 for silicon at low frequencies[44]), ε_0 is the vacuum permittivity (8.85×10^{-12} F m^{-1}), and N is the homogenous doping density in the semiconductor (m^{-3})—typically in the range 10^{20}–10^{26} m^{-3} (i.e., 10^{14}–10^{20} cm^{-3}) for silicon.

The charge associated with the insulator layer Q_i is given by

$$Q_i = \beta V_i, \tag{6}$$

$$\beta = \frac{\varepsilon_i \varepsilon_0}{t_i}, \tag{7}$$

where ε_i is the dielectric constant of the insulator (e.g., ~2 and 3.9 for amorphous fluoropolymers[23] and silicon dioxide[44] at low frequencies) and t_i is the thickness of the dielectric (typically 100–1000 nm).

In terms of the EDL at high voltages,[38–43] if $V_e \gg kT/q$ (k is the Boltzmann constant 1.38×10^{-23} J K^{-1} and T is the temperature of the junction—in Kelvin), then it has been shown[38,41,43] that the charge at the electrolyte-insulator interface Q_e can be approximated by

$$Q_e \approx \delta\sqrt{V_e}, \tag{8}$$

where

$$\delta = C_0\sqrt{\frac{2}{\rho}}, \tag{9}$$

where ρ is the ratio of the total number of anions and cations in the bulk to the total number of available sites at the interface[38]—($0 \le \rho \le 1$)—N.B. depending on the nature of the electrolyte, the value of ρ can be dependent on the concentration and the polarization.[38] C_0 is the zero bias capacitance of the EDL and is given by $\varepsilon_e\varepsilon_0/4\pi L_D$, where ε_e is the low frequency dielectric constant of the electrolyte (e.g., 50–80 for aqueous solutions)[45] and L_D is the Debye length $\sqrt{\varepsilon_e\varepsilon_0 kT/4\pi q^2 z^2 N_A c}$, where z is the valence of the ion species, N_A is the Avogadro constant (6.02×10^{23} mol^{-1}), and c is the bulk molar concentration of the electrolyte (mol m^{-3}).

We are now in a position to rearrange Eqs. (4), (6), and (8)—by assigning a charge Q and using Eq. (3)—in order to obtain the following quadratic formula:

$$\left(\frac{1}{\alpha^2} + \frac{1}{\delta^2}\right)Q^2 + \frac{1}{\beta}Q - V = 0, \tag{10}$$

which has the following solutions for Q

$$Q = \frac{\alpha\delta(-\alpha\delta + \sqrt{\alpha^2\delta^2 + 4\beta^2\delta^2 V + 4\beta^2\alpha^2 V})}{2\beta(\alpha^2 + \delta^2)}. \tag{11}$$

This equation can be integrated with respect to V to obtain a formula for the stored energy E of the EIS junction as a function of applied voltage V

$$E = \frac{\alpha\delta\left(-\alpha\delta V + \frac{2}{3}\frac{\left((4\beta^2\delta^2 + 4\beta^2\alpha^2)V + \alpha^2\delta^2\right)^{\frac{3}{2}}}{4\beta^2\delta^2 + 4\beta^2\alpha^2}\right)}{2\beta(\delta^2 + \alpha^2)} + K. \tag{12}$$

In order to obtain the integration constant K, we make the assumption that at $V = 0$, E is approximately zero

$$K = -\frac{\alpha^4\delta^4}{12\beta^3(\alpha^2 + \delta^2)^2}. \tag{13}$$

Equations (1), (12), and (13) can now be combined to give a modified Young-Lippmann equation for EW at an EIS junction *when the semiconductor is in depletion*.

In the case where the semiconductor is in accumulation—e.g., a negative voltage for a p-type semiconductor—then it is reasonable to assume that V_{sc} and $Q_{sc} = 0$. By following the same reasoning as above it can be shown that

$$E = \frac{\delta\left(-\delta V + \frac{(\delta^2 + 4\beta^2 V)^{\frac{3}{2}}}{6\beta^2}\right)}{2\beta} - \frac{\delta^4}{12\beta^3}. \tag{14}$$

Equations (1) and (14) can now be combined to give a modified Young-Lippmann equation for EW at an EIS junction *when the semiconductor is in accumulation*. Note also that the model does not take into account—high field effects in the semiconductor,[44] effects at the semiconductor-insulator interface (e.g., traps),[44] electrical breakdown in the semiconductor, insulator, or electrolyte, other complications associated with the electrolyte and EDL, e.g., electrochemistry at the electrolyte-insulator interface[38,40,42] and high frequency effects.

EW experiments were conducted in order to test the model. Single crystal polished (100) silicon wafers, having differing resistivity and doping types, were spin coated with an amorphous fluoropolymer layer (Teflon®AF, Dupont, USA). The doping densities of the silicon were[25] 5.2×10^{14} cm^{-3} (n-type), 2.1×10^{15} cm^{-3} (p-type), 3.5×10^{17} cm^{-3} (n+ type), and 8×10^{18} cm^{-3} (p+ type). Ohmic contacts were formed on the rear surfaces of the silicon using ion implantation (10^{20} cm^{-3}), aluminum evaporation and heat treatment[23]—this is an important point in order to avoid diode like behavior (voltage polarity asymmetry) not related to the EIS junction. The thickness of the amorphous fluoropolymer was used 265 nm. For a typical EWOD insulator thickness of >1 μm the areal capacitances of the dielectric layer (assuming $\varepsilon_i \sim 2$) and the EDL layer only become comparable for solution concentrations of <1 nM—i.e., for most common electrolyte concentrations the EDL effect will not be observed. Aqueous HCl solutions (10 mM–1 nM) were prepared using electronic grade (RSE) HCl (37%) (Carlo-Erba, France) and deionized water—HCl is a uni-univalent electrolyte, yielding H^+ and Cl^- in solution. The samples and solutions were prepared, and the experiments were conducted, in a class ISO 5/7 cleanroom ($T = 20\,°C \pm 0.5\,°C$; RH = 45% ± 2%) environment. The details of the EW setup have been described elsewhere.[23] The applied voltage was ramped to ±30 V at a ramp rate of ~1–2 V s^{-1} using an

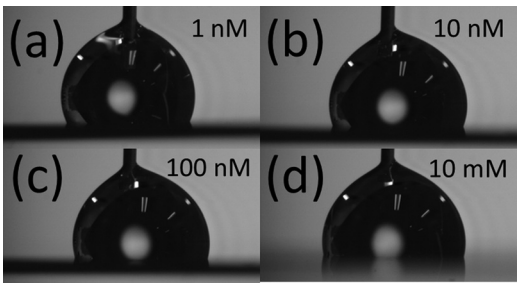

FIG. 2. EW at an EIS junction—effect of electrolyte concentration when the semiconductor is in depletion. (a) 1 nM HCl at +30 V, (b) 10 nM HCl at +30 V, (c) 100 nM HCl at +30 V, and (d) 10 mM HCl at +30 V. The semiconductor is p+ type silicon (8×10^{18} cm^{-3}) and the insulator is a 265 nm thick amorphous fluoropolymer (Teflon®AF). The diameter of the needle is 300 μm.

E3634A DC power supply (Agilent, USA). The droplet shape data were gathered using a commercial Contact Angle Meter (GBX Scientific Instruments, France). The contact angles were extracted from the photographs using a digitized algorithmic method.[46]

Fig. 1 shows the effect of doping density and doping type of the silicon wafers on the EW at an EIS junction using an aqueous HCl solution having a concentration of 10 mM using a p+ type [Fig. 1(a)] and a p-type wafer [Fig. 1(b)]—correspond to an aqueous HCl solution having a concentration of 10 mM using a n+ type [Fig. 1(c)] and a n-type wafer [Fig. 1(d)]. Droplets having an HCl concentration of 10 mM were used to ensure that the EW is dominated by space-charge effects in the semiconductor and the insulator capacitance. The doping density and type has a role in the EW behavior—the droplet is observed to spread out more upon application of the voltage (±30 V) when the semiconductor is in accumulation. Fig. 2 shows the effect of changing the electrolyte concentration on the EW at an EIS junction. When the highly doped semiconductor is in depletion, the droplet is observed to spread out less upon application of a voltage (±30 V) in the case of a lower molarity solution [Fig. 2(d)]—suggesting the influence of the EDL.

Fig. 3 shows plots of the contact angle of the droplet versus applied voltage at an EIS junction for the four types of silicon wafers. Repeated measurements were conducted

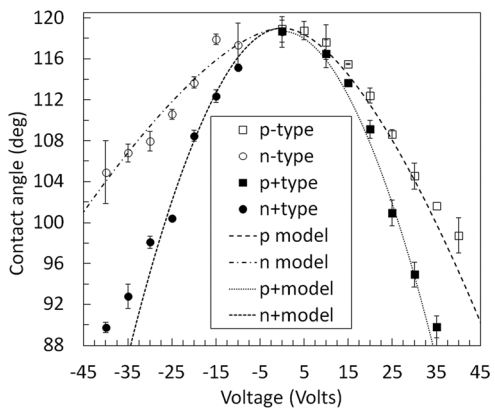

FIG. 3. Effect of semiconductor doping on EW at an EIS junction. Experimental EW at an EIS junction using a relatively high molarity electrolyte solution (10 mM) for different doping density silicon wafers coated with 265 nm thick amorphous fluorocarbon.[23] Solid symbols correspond to highly doped silicon—open symbols correspond to lowly doped silicon.

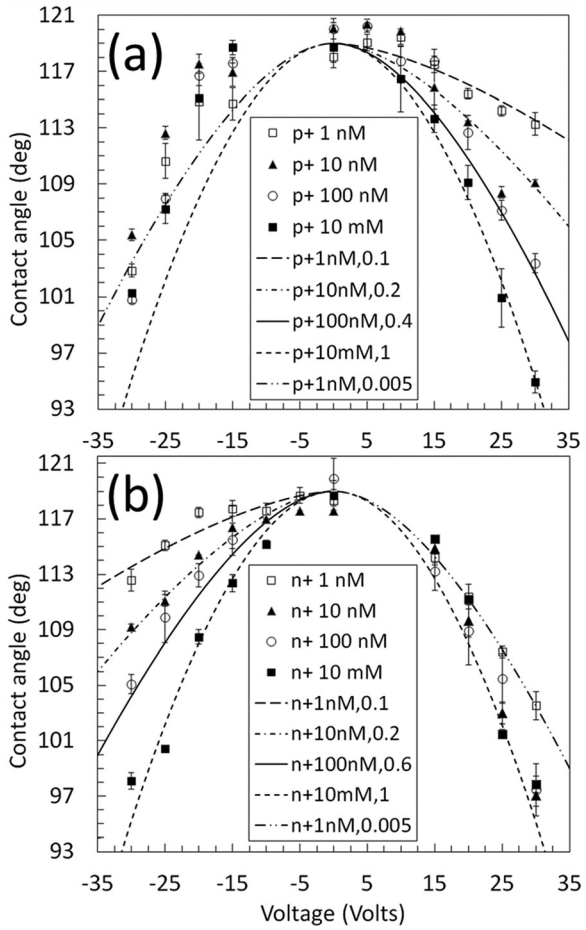

FIG. 4. Effect of electrolyte concentration on electrowetting at an EIS junction. Experimental EW at an EIS junction using low molarity electrolyte (10 mM–1 nM) using (a) p+ doped silicon wafers coated with a 265 nm thick amorphous fluorocarbon and (b) n+ doped silicon wafers coated with a 265 nm thick amorphous fluorocarbon. Open squares—1 nM, solid triangles—10 nM, open circles—100 nM and solid squares—10 mM. The number given in the legend corresponds to the value of ρ.

using the same fluoropolymer coated silicon wafers already published[23]—allowing the inclusion of error bars and a comparison with the model presented here—see later. In the case of high doping (solid symbols), the EW behavior is EWOD-like (i.e., $\theta \sim V^2$) due to the fact that the space-charge layer in the highly doped silicon will be very small—i.e., high capacity—allowing the insulator capacitance to dominate the EW. In the case of low doping (open symbols), the evolution of the contact angle is markedly less due to the influence of the space-charge at the semiconductor-insulator interface which now dominates over the insulator capacitance. The effect of the semiconductor space-charge has been previously observed[23] using high electrolyte concentrations (c > 1 mM)—in this case, the contribution of the EDL capacitance can be neglected due to a very small Debye length ~10 nm. This is not the case in the following where the electrolyte concentration is reduced to <1 mM.

Fig. 4 shows the effect of electrolyte concentration on the EW behavior of an EIS junction. Droplets having an HCl concentration varying from 10 mM to 1 nM and highly doped n-type and p-type silicon wafers were used to ensure that the EW is dominated by effects at the electrolyte-insulator interface. Fig. 4(b) corresponds to p+ type silicon—Fig. 4(b) corresponds to n+ type silicon. First, when the silicon is in

depletion the effect of the solution concentration is evident—a lower concentration resulting is a smaller EW response. A high molarity (10 mM—solid squares) results in an EWOD-like EW response (i.e., $\theta \sim V^2$), whereas a low molarity (1 nM—open squares) results in a diminished EW response—this is as much as 16° for both doping types at ±30 V. The EW response of droplets having intermediate concentrations falls within these values. The zero bias contact angle θ_0 changes little (<2°) over the solution concentrations studied. Two comments on the voltage magnitude and polarity: first, the voltages used are sufficient to observe EW but not high enough to observe contact angle hysteresis (CAS).[47] Second, using voltages which cause accumulation in the silicon wafers, the effect of the electrolyte concentration on the EW response become less evident and the data become noisier—especially for the p+ type wafer.

Let us now look at how the predictions of the model fit the experimental data. The curves in Figs. 3 and 4 are based on Eqs. (1), (12), (13), and (14) using the following physical parameters: $\varepsilon_{Si} = 11.9$,[44] $\varepsilon_{Tef} = 1.92$,[23] $\varepsilon_{HCl} = 80$,[48,49] $\gamma_{HCl} = 72.8\,\mathrm{mJ\,m^{-2}}$,[50] $z_{HCl} = 1$, $T = 300\,\mathrm{K}$, and $z = 1$. All the physical parameters of the model are very well known, except the value of ρ—which is thought to be both concentration and voltage-polarity dependent.[38] In order to fit the model to the experimental contact angle values, the value of ρ has been varied—although it is not a free parameter.

The theoretical model fits the experimental data very well for voltages causing depletion *and* accumulation in the silicon of differing doping densities and types; accurately predicting that the reduction of the contact angle of a high concentration electrolyte (10 mM)—Fig. 3. Let us now consider the curves in Fig. 4. Let us first consider voltages which cause depletion in the silicon. The experiments indicate that the model is able to accurately predict the *range* of molar concentration over which the EW becomes dominated by the effect of the EDL—this occurs between 100 nM and 1 nM—as is indeed observed in the experiments. This indicates that the high voltage capacitance model[38] given in Eqs. (8) and (9) is relatively accurate for the voltage range—and the electrolyte—used here in the experiments. As stated above, although it is not a free parameter the value of ρ needs to be adjusted to fit the model to the experimental data, indicating—as previously suggested[38]—that the value of ρ would appear to be concentration dependent and to a certain extent, voltage-polarity dependent. These results are in agreement with EW observations using varying electrolyte concentration.[17–21] In the case of high electrolyte concentration, i.e., 10 mM, the value of ρ is set to 1 for both doping types. For $c = 1$ nM, the value of ρ is set to 0.1—for $c = 10$ nM, the value of ρ is set to 0.2—in the case of p-type silicon, for $c = 100$ nM, the value of ρ is set to 0.4. For n-type material and for 100 nM, the value of ρ needs to be set a little higher (0.6) to fit the experimental data—suggesting a voltage-polarity related effect. When the applied voltage causes accumulation in the silicon, the value of ρ used for depletion no longer fits the contact angle data. For example, in order to fit the n+ type data using a 1 nM solution in accumulation, i.e., a positive voltage, the value of ρ needs to be set to 0.005—indicating that either the value of ρ is highly voltage polarity dependent or that there is another factor not included in the model which is coming into play, e.g., breakdown in the insulator. Finally, note that the experiments—if performed carefully—could, in principle, be used to obtain the value of ρ for various electrolytes; the experiments here indicate that the value of ρ decreases with decreasing H^+ and Cl^- concentration—under both positive and negative voltage polarities.

[1]F. Mugele and J.-C. Baret, J. Phys. Condens. Matter **17**, R705 (2005).
[2]W. C. Nelson and C. J. Kim, J. Adhes. Sci. Technol. **26**, 1747 (2012).
[3]G. Beni, Appl. Phys. Lett. **38**, 207 (1981).
[4]M. G. Pollack, R. B. Fair, and A. D. Shenderov, Appl. Phys. Lett. **77**, 1725 (2000).
[5]H. J. Lee and C.-J. Kim, J. Microelectromech. Syst. **9**, 171 (2000).
[6]B. Berge and J. Peseux, Eur. Phys. J. E **3**, 159 (2000).
[7]T. Krupenkin, S. Yang, and P. Mach, Appl. Phys. Lett. **82**, 316 (2003).
[8]R. A. Hayes and B. J. Feenstra, Nature **425**, 383 (2003).
[9]H. You and A. J. Steckl, Appl. Phys. Lett. **97**, 023514 (2010).
[10]A. R. Wheeler, Science **322**, 539 (2008).
[11]T. Krupenkin and J. A. Taylor, Nat. Commun. **2**, 448 (2011).
[12]X. Feng, B.-F. Liu, J. Li, and X. Liu, "Advances in coupling microfluidic chips to mass spectrometry," Mass Spectrom. Rev. **33**, 1 (published online 2014).
[13]T. Liu, P. Sen, and C.-J. Kim, J. Microelectromech. Syst. **21**, 443 (2012).
[14]B. Berge, C. R. Acad. Sci., Ser. II: Mec., Phys., Chim., Sci. Terre Univers **317**, 157 (1993).
[15]H. J. J. Verheijen and M. W. J. Prins, Langmuir **15**, 6616 (1999).
[16]V. Peykov, A. Quinn, and J. Ralston, Colloid Polym. Sci. **278**, 789 (2000).
[17]A. Quinn, R. Sedev, and J. Ralston, J. Phys. Chem. B **107**, 1163 (2003).
[18]L. Zhu, J. Xu, Y. Xiu, Y. Sun, D. W. Hess, and C.-P. Wong, J. Phys. Chem. B **110**, 15945 (2006).
[19]A. A. Kornyshev, A. R. Kucernak, M. Marinescu, C. W. Monroe, A. E. S. Sleightholme, and M. Urbakh, J. Phys. Chem. C **114**, 14885 (2010).
[20]C.-P. Lee, B.-Y. Fang, and Z.-H. Wei, Analyst **138**, 2372 (2013).
[21]L. Chen, C. Li, N. F. van der Vegt, G. Auernhammer, and E. Bonaccurso, Phys. Rev. Lett. **110**, 026103 (2013).
[22]D. C. Grahame, Chem. Rev. **41**, 441 (1947).
[23]S. Arscott, Sci. Rep. **1**, 184 (2011).
[24]S. Arscott, Appl. Phys. Lett. **103**, 144101 (2013).
[25]S. Arscott and M. Gaudet, Appl. Phys. Lett. **103**, 074104 (2013).
[26]S. Arscott, RSC Adv. **4**, 29223 (2014).
[27]M. Grätzel, Inorg. Chem. **44**, 6841 (2005).
[28]F. Buth, D. Kumar, M. Stutzmann, and J. A. Garrido, Appl. Phys. Lett. **98**, 153302 (2011).
[29]C. Pietzka, G. Li, M. Alomari, H. Xing, D. Jena, and E. Kohn, J. Appl. Phys. **112**, 074508 (2012).
[30]V. H. Velez, R. G. Mertens, and K. B. Sundaram, in 224th ECS Meeting, San Francisco, CA, 27 October–1 November, 2013.
[31]X. Zhang, A. Hosseini, X. Lin, H. Subbaraman, and R. T. Chen, IEEE J. Sel. Top. Quantum Electron. **19**, 196 (2013).
[32]T. B. Jones, Langmuir **18**, 4437 (2002).
[33]H. Wang and L. Pilon, J. Phys. Chem. C **115**, 16711 (2011).
[34]W. M. Siu and R. S. Cobbold, IEEE Trans. Electron Devices **26**, 1805 (1979).
[35]C. D. Fung, P. W. Cheung, and W. H. Ko, IEEE Trans. Electron Devices **33**, 8 (1986).
[36]M. Dhindsa, S. Kuiper, and J. Heikenfeld, Thin Solid Films **519**, 3346 (2011).
[37]E. Bormashenko, R. Pogreb, Y. Bormashenko, R. Grynyov, and O. Gendelman, Appl. Phys. Lett. **104**, 171601 (2014).
[38]A. A. Kornyshev, J. Phys. Chem. B **111**, 5545 (2007).
[39]M. Kilic, M. Bazant, and A. Ajdari, Phys. Rev. E **75**, 021502 (2007).
[40]M. V. Fedorov and A. A. Kornyshev, J. Phys. Chem. B **112**, 11868 (2008).
[41]M. V. Fedorov and A. A. Kornyshev, Electrochim. Acta **53**, 6835 (2008).
[42]M. Z. Bazant, M. S. Kilic, B. D. Storey, and A. Ajdari, New J. Phys. **11**, 075016 (2009).
[43]M. Z. Bazant, B. D. Storey, and A. A. Kornyshev, Phys. Rev. Lett. **106**, 046102 (2011).
[44]S. M. Sze and K. K. Ng, *Physics of Semiconductor Devices*, 3rd ed. (Wiley-Interscience, Hoboken, 2007).
[45]B. E. Conway, J. O. Bockris, and I. A. Ammar, Trans. Faraday Soc. **47**, 756 (1951).
[46]A. F. Stalder, G. Kulik, D. Sage, L. Barbieri, and P. Hoffmann, Colloids Surf., A **286**, 92 (2006).
[47]F. Mugele, Soft Matter **5**, 3377 (2009).
[48]J. B. Hasted and G. W. Roderick, J. Chem. Phys. **29**, 17 (1958).
[49]A. S. Lileev, D. V. Loginova, and A. K. Lyashchenko, Mendeleev Commun. **17**, 364 (2007).
[50]P. K. Weissenborn and R. J. Pugh, J. Colloid Interface Sci. **184**, 550 (1996).